American Mineralogist, Volume 84, pages 517–527, 1999

Peristerite exsolution in metamorphic plagioclase from the Lepontine Alps: An analytical and transmission electron microscope study

DAWN E. JANNEY* AND HANS-RUDOLF WENK

Department of Geology and Geophysics, University of California, Berkeley, California 94720, U.S.A.

ABSTRACT

Transmission and analytical electron microscopy were used to examine relationships between microstructures and compositions in greenschist- and amphibolite-facies metamorphic plagioclase (albite and oligoclase) from the Lepontine Alps (Switzerland and Italy). Two kinds of exsolution microstructures related to the peristerite miscibility gap ($\sim An_{1-25}$) were observed: lamellae, in bulk compositions ranging from a few mole percent anorthite to $\sim An_{10-15}$, and tweeds, in bulk compositions from almost pure albite to $\sim An_{15-18}$. Lamellae are typically 15 to 35 nm thick. Individual lamellae in crystallographically homogeneous or tweedy areas commonly have highly irregular spacings or end at dislocations or subgrain boundaries, suggesting formation by heterogeneous nucleation. Tweeds are characteristically diffuse, and probably formed by spinodal decomposition. Many tweeds have one exsolution direction that is consistently sharper or coarser than the other. Tweeds and lamellae may be intergrown in patches with irregular, curving boundaries, some of which define narrow stripes several micrometers long. Exsolution directions in these tweeds are approximately parallel and perpendicular to the lamellae. The perpendicular direction is usually less diffuse or more regular than the parallel direction, and may continue between widely spaced individuals in patches of lamellae. Tweeds in these intergrowths appear to be slightly more sodic than adjacent areas with lamellae.

Except near fractures and in areas with high dislocation densities, differences in microstructures within a single grain almost invariably reflect differences in composition. Microstructural variability within single grains, and among different grains from the same hand sample, was so large that it was impossible to identify systematic relationships between microstructures and metamorphic grade.

INTRODUCTION

The plagioclase feldspars form a complete high-temperature solid solution between albite ($NaAlSi_3O_8$) and anorthite ($CaAl_2Si_2O_8$). At lower temperatures, there are three generally recognized miscibility gaps (e.g., Carpenter 1994; Smith and Brown 1988), of which the peristerite gap ($\sim$1–25 mol% anorthite) is the most sodic. It is interpreted as a conditional solvus and spinodal, occurring because of the much greater reduction in free energy resulting from Al,Si-ordering in pure albite than in slightly more calcic compositions (Carpenter 1981; Brown 1989; Carpenter 1994).

Numerous field observations of albite and oligoclase coexisting in apparent equilibrium are in general agreement about the highly asymmetric shape of the peristerite gap (e.g., Crawford 1966; Maruyama et al. 1982; Grapes and Otsuki 1983; Ashworth and Evirgen 1985). The sodic limb is almost pure albite, whereas the calcic limb slopes from the crest (probably $\sim An_{10}$, and close to the greenschist-amphibolite facies transition in moderate-pressure regional metamorphism) to $\sim An_{25}$.

Optical, X-ray diffraction (XRD), and transmission electron microscopy (TEM) studies of peristerites have shown two distinct types of exsolution microstructures occurring in different bulk compositions. Exsolved peristerites between $\sim An_1$ and $\sim An_{16-17}$ have parallel lamellae, typically several tens to hundreds of nanometers thick, which commonly have sharp boundaries (e.g., Fleet and Ribbe 1965; Lorimer et al. 1974; McLaren 1974; Olsen 1974; Olsen 1975; Brown 1989; Baschek and Eberhard 1995). Single-crystal XRD patterns characteristically show two reciprocal lattices, with lattice angles corresponding to albite and oligoclase ($\sim An_{17-30}$) (e.g., Laves 1954; Brown 1960; Baschek and Eberhard 1995). Ion microprobe measurements confirm that the lamellae are albite and oligoclase (Miúra and Rucklidge 1979).

In contrast, XRD and electron diffraction studies of peristerites from $\sim An_{16}$ to $\sim An_{25}$ show only one crystal lattice (Laves 1954; Brown 1960; Fleet and Ribbe 1965; Korekawa et al. 1970). TEM studies show fine microstructures with two intersecting directions (Korekawa et al. 1970; McLaren 1974; Nord et al. 1978).

* Present address: Department of Geology, Arizona State University, P.O. Box 871404, Tempe, Arizona 85287-1404, U.S.A. E-mail: djanney@asu.edu

0003–004X/99/0004–0517$05.00

Both kinds of exsolution microstructures are generally believed to form by spinodal decomposition (e.g., Nord et al. 1978; Brown 1989). It has been conjectured that tweeds are the primary exsolution microstructure in all peristerite compositions, and that lamellae form in sodic peristerites when one direction of the tweeds coarsens and the other disappears (Champness and Lorimer 1976). However, microstructures interpreted to represent intermediate stages of coarsening have not been observed in compositions in which lamellae would be expected.

Almost all previously studied peristerites have been fairly homogeneous single crystals of slowly cooled, high-temperature igneous and metamorphic plagioclase. Low-temperature exsolution kinetics are exceedingly sluggish, and experimentally measured high-temperature Al-Si interdiffusion constants cannot be extrapolated to low temperatures without implying implausibly long durations for formation of the observed microstructures (Carpenter 1994; Brown 1989; Wruck and Salje 1991 and included older references). In principle, lower-grade metamorphic plagioclases should also be valuable sources of information; in practice, however, complicating factors such as small-scale chemical heterogeneity, an apparently widespread tendency to crystallize in metastably disordered states, and a chaotic distribution of coexisting compositions (summarized in Carpenter 1994) make studies of exsolution processes in metamorphic plagioclases quite difficult, and published results are rare.

The research reported here uses a combination of transmission and analytical electron microscopy (TEM and AEM) to study greenschist- and amphibolite-facies metamorphic peristerites from the Central Alps. Microstructures are commonly variable on a scale of a few micrometers or tenths of micrometers, and chemical analyses using AEM made it possible to examine relationships between microstructures and local bulk compositions. The samples in this study contain very sodic tweeds and intergrowths of tweeds and lamellae (neither of which has been previously reported to our knowledge), and thus provide new information about both the mechanisms involved in peristerite exsolution and the relationships between composition and exsolution microstructures.

Experimental methods

Single plagioclase grains from nine hand specimens of amphibolite, calc-silicate, and gneiss from the Lepontine Alps (Fig. 1) were selected from the collections of E. Wenk (Mineralogisch-Petrographisches Institut, Universität Basel, Switzerland) and H.-R. Wenk (University of California, Berkeley). The hand specimens were chosen on the basis of previously published studies and unpublished optical and microprobe composition determinations (Table 1). Many of the specimens also contain compositions more calcic than $\sim An_{25}$, which are not considered here.

Individual plagioclase grains were selected from each hand specimen based on optical examination of 30 μm thick sections. Each sample was glued to a 3 mm diameter copper grid, ion-milled to electron transparency, and coated with a thin layer of carbon. Large crystals with patchy extinction were preferred because it seemed possible that the extinction resulted from compositional zoning, allowing comparison of microstructures in different compositions with presumably very similar metamorphic histories.

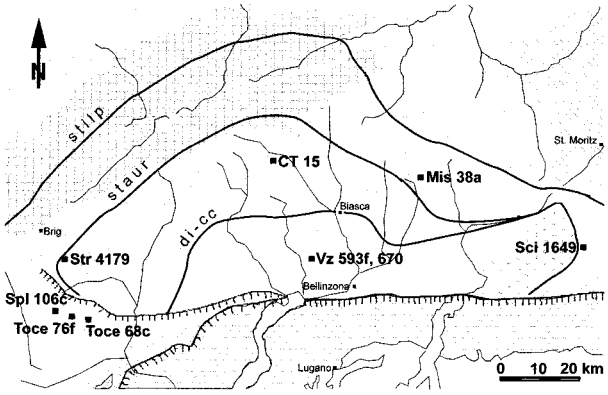

Figure 1. Schematic geologic map of the Lepontine Alps showing locations of samples in this study (base map and isograds after Frey et al. 1983). The ''stilp,'' ''staur,'' and ''di-cc'' lines indicate positions of the stilpnomelane-out, staurolite-in, and diopside + calcite-in mineral zone boundaries or reaction isograds. The''staur'' line coincides with the first appearance of andesine ($\sim An_{30}$) and the closure of the peristerite gap (Wenk and Wenk 1984). Metamorphic conditions reached 600–650 °C and 6–7 kb at Campo Tencia (CT 15), and 650–700 °C and 3–5 kb near Bellinzona (Frey et al. 1980). Other symbols: cross-hatched = Aar and Gotthard Massifs; gray = Mesozoic and Neogene Pennine sediments; blank = other Pennine rocks; broken diagonals = east Alpine nappes; horizontal dashes = southern Alps; crosses = Bergell intrusive; lines with tick marks = Insubric Line and Simplon-Centovalli Fault.

With the exception of specimen Sci 1649, the selected grains from the amphibolites and calc-silicates are probably porphyroblasts that formed during the main Tertiary Lepontine metamorphism (10–30 Ma; Hunziker et al. 1989). Host rocks were originally basaltic rocks and silicic sediments from a Triassic-Jurassic geosynclinal basin to the north of the present Alps (Coward and Dietrich 1989; Wenk and Wenk 1984). The grain from Sci 1649 is a re-metamorphosed phenocryst from a sample that previously had been shown to contain compositions ranging from albite to anorthite within a single grain (Wenk 1979).

Compositions and microstructures were observed with a combination of conventional TEM and AEM. TEM was done with a JEOL JEM 100C at the University of California, Berkeley, operating at 100 kV, and with the JEOL JEM 200CX Analytical Electron Microscope at the National Center for Electron Microscopy, Ernest Orlando Lawrence Berkeley National Laboratory, operating in TEM mode at 200 kV. Both microscopes have high-tilt stages: a ±45°/>360° tilt-rotate stage for the 100C and a ±30°/±60° double-tilt stage for the 200CX.

Quantitative chemical data was collected using the Analytical Electron Microscope in STEM mode, rastering the beam over the largest rectangular area that was con-

TABLE 1. Sample descriptions

Sample number	Location (Swiss coordinates)	Description	References
Vz 670	Verzasca (712.1/123.98)	Weakly foliated quartz-plagioclase-microcline-gneiss with biotite, muscovite, chlorite.	
Vz 593f	Verzasca (712.1/124.0)	Quartz-plagioclase (~An_{25} and An_{32})-biotite gneiss with garnet, kyanite.	Wenk and Wenk 1977
CT 15	Campo Tencia (700/142.7)	Kyanite-garnet-quartz-alkali feldspar-plagioclase lens in gneiss. Has optically visible intergrowths of two plagioclase compositions (~An_{20} and An_{40}), of which only the An_{20} is considered here.	
Sci 1649	Cavloccio (774.6/138.7)	Metamorphosed phenocryst in actinolite-pargasite schist; contains albite, anorthite, and intermediate compositions.	Wenk 1979
Mis 38a	Mesolcina (735.4/145.4)	Calcareous schist with muscovite, opaques, quartz, 2 plagioclases (An_{0-3} + An_{18-26}), sphene.	
Str 4179	Kaltwasserpass (~649.0/123.1)	Biotite-calcite-quartz-plagioclase (albite + An_{13-19}) gneiss with accessory muscovite and rare opaque minerals.	Streckeisen and Wenk 1974
Spl 106c	Antrona (652.2/106.5)	Hornblende-clinozoisite-chlorite amphibolite with plagioclase (albite, oligoclase), apatite, calcite, sphene, opaques, quartz.	Wenk and Keller 1969
Toce 68c	NW Villadossola (659.75/104.5)	Amphibolite with 2 plagioclases (An_4 + An_{25-28}), biotite, chlorite, epidote, carbonate, sphene, and quartz.	Wenk and Keller 1969
Toce 76f	Bognanco (656.5/108.8)	Strongly foliated amphibolite with 2 plagioclases (albite + An_{29-36}), epidote, actionlite or actinolitic hornblende, sphene, rutile, and rare opaques.	Wenk and Keller 1969

Notes: Samples are arranged in roughly decreasing order of metamorphic grade (corresponding to Fig. 2). Plagioclase compositions are from optical and microprobe techniques (see Fig. 2 for AEM data). We thank E. Wenk for his kind permission to include his unpublished data.

sistent with maintaining a uniform specimen thickness (typically a few hundred nanometers per side) to produce an approximate average composition of finer-scale exsolution microstructures. All of the data was collected with the specimen cooled by liquid nitrogen. Other data-collection practices evolved during the research, as increasingly beam-sensitive specimens were encountered. Measures used to reduce beam damage included reducing current density by increasing the beam size and undersaturating the filament, and combining data from larger areas with similar microstructures by moving to a new area as soon as beam damage became evident. However, it was usually impossible to measure compositions without damaging the microstructures.

X-rays were collected using a Kevex solid-state detector with a 72° take-off angle and 5 μm thick beryllium window. All X-ray spectra were examined visually for characteristic peaks from elements with atomic numbers from 11 (Na) through 30 (Zn). Na, Al, Si, and Ca were assumed to be entirely from the samples. Each analysis also shows some Cu (probably mostly from the grid). Peaks indicating traces of S, Cl, Ar, Cr, Fe, and K also were observed in a few cases. The S, Cl, Ar, Cr, and perhaps Fe are interpreted as sample-preparation artifacts. The K is more difficult: although it is a likely trace element in plagioclase, almost all of the analyses in this study that have recognizable K also have larger quantities of S and Cl, and the relationship between the heights of the K, Cl, and S peaks is sufficiently consistent to suggest that much of the K in this study also may be a sample-preparation artifact. In any case, there does not appear to be a consistent relationship between K contents and microstructures.

Atomic percentages of Na, Al, Si, and Ca were obtained with Kevex Temstar software (version 3.09) using an empirical background correction and Gaussian deconvolution. With the exception of Vz 593 data, all spectra were deconvoluted for Na, Al, Si, and Ca (if present). Vz 593 spectra were mistakenly deconvoluted as though K were present. Comparisons of similar spectra deconvoluted with and without K show no recognizable effect on the final composition determinations.

Theoretical k-factors were used to quantify elemental concentration ratios. Atomic percentages for each spectrum were re-normalized to Al + Si = 4, and mole fractions of anorthite were calculated from the Na/(Al + Si), Al/(Al + Si), and Ca/(Al + Si) ratios. In many cases, anorthite contents calculated from Na often differed from those calculated from Al and Ca by at least 10–15 mol%. At least two factors probably contribute to these differences: first, the well-known mobility of Na in the AEM environment (e.g., Mackinnon 1990; Peacor 1992); and second, the inability of the detector to resolve the energy overlap between Cu*L* and Na*K* characteristic X-rays. Because of these factors, anorthite contents from Na were not utilized in data interpretation.

AEM ANALYSES AND MICROSTRUCTURE-COMPOSITION RELATIONSHIPS

Figure 2 shows AEM analyses and their relationships to microstructures. In almost all cases, the mole fraction of anorthite calculated from the Al/(Al + Si) ratio is low-

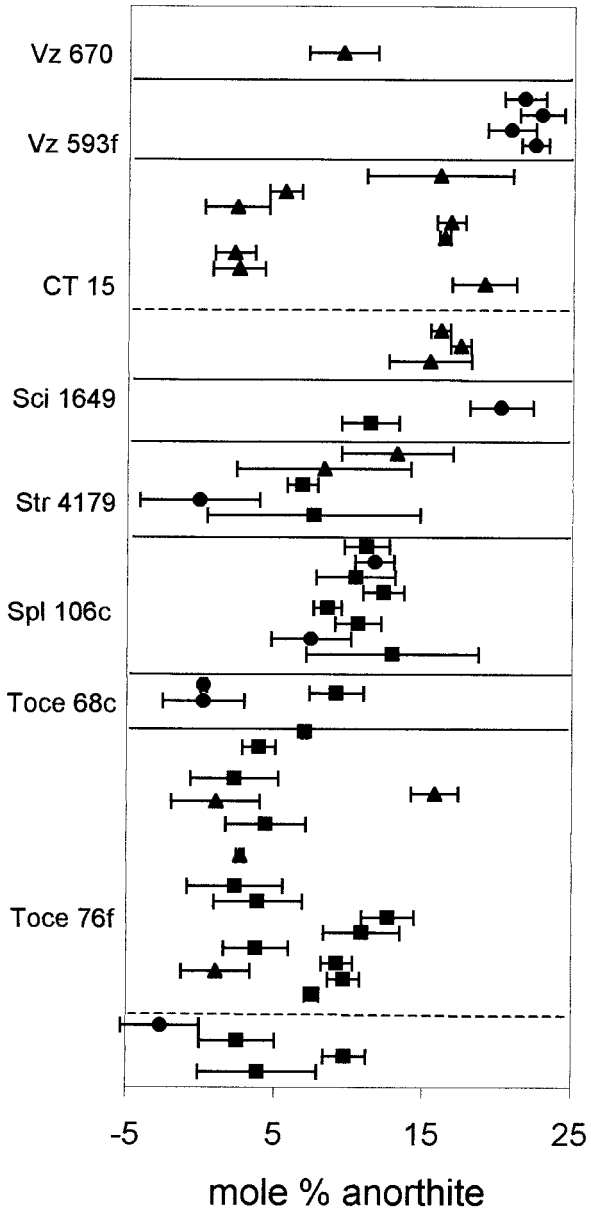

FIGURE 2. Results of AEM analyses and composition-microstructure relationships. Each data point represents the average mole percent anorthite determined from the Al/(Al + Si) ratio and from the Ca/(Al + Si) ratio for one AEM analysis. Negative mole percentages of anorthite represent analyses with less Al than is in pure albite. Horizontal bars are not true error bars, but indicate the difference between the compositions determined from each ratio. Symbols indicate the associated microstructures: squares for lamellae, triangles for tweeds, and circles for areas without exsolution microstructures. Samples are arranged in approximate increasing order of metamorphic grade. Horizontal dotted lines separate different grains from a single hand sample; otherwise, all analyses are from a single grain per specimen. Vertical positions within the data for each grain are arbitrary.

er than that from the Ca/(Al + Si) ratio, and analyses of some very sodic plagioclases show less Al than is present in normal albite. Microprobe analyses of similar plagioclases from the Central Alps (e.g., Wenk et al. 1977; Wenk et al. 1991) do not show a corresponding pattern of differences between mole fractions of anorthite calculated from Al/(Al + Si) and from Ca/(Al + Si). Thus, it seems possible that the anomalously low Al in the AEM analyses may result from electron-beam-induced sample damage during analysis. Yund and Tullis (1991) and Mackinnon (1990) also report similar apparent losses of Al during AEM analysis of plagioclase.

Other possible sources of error in the data in Figure 2 include imperfect matches between the Gaussian deconvolutions and the spectra, and errors due to counting statistics. The lack of a systematic trend in the differences between compositions from Al and Ca as a function of composition suggests that the k-factors are not a major source of error.

Figure 2 classifies microstructures as lamellae, in which one exsolution direction was observed, or tweeds, in which two were seen. Areas in which no exsolution microstructures were observed are also shown. Lamellae were generally quite easy to recognize, and were visible from a wide range of tilts. In many cases, tweeds often changed appearance significantly with small differences in sample orientation, and both directions of fine, diffuse tweeds were only visible from a very restricted range of sample tilts. Although each specimen was tilted extensively, it is impossible to rule out the existence of exsolution directions that were not observed because of sample geometry (e.g., exsolution directions oriented parallel to the plane of the specimen).

Lamellae occur only in compositions with at least a few mole percent anorthite, but not in compositions more calcic than $\sim An_{10-15}$. Tweeds occur from almost pure albite to $\sim An_{15-20}$, overlapping the entire compositional range of the lamellae. Lamellae were not observed in the highest-grade samples, but there is otherwise no consistent pattern relating the presence or absence of tweeds and lamellae to metamorphic grade. (As mentioned above, many previously studied lamellae are found in high-temperature plagioclases. Thus, the absence of lamellae here cannot be interpreted as a consequence of metamorphic grade.)

Several samples contain more than one kind of peristerite microstructure. In Toce 76f, homogeneous plagioclases are pure albite, whereas the more sodic tweeds are intergrown with slightly more calcic lamellae; there is also an isolated patch of tweed that is significantly more calcic. Str 4179 follows a somewhat different pattern, in which large areas of lamellae and tweeds occur in different parts of the same crystal. The two distinct tweed compositions in CT 15 also occur in separate areas. In addition to the tweed shown, Vz 670 has extensive areas of essentially pure albite, as well as peristerite compositions ranging from $\sim An_2$ to $\sim An_{10}$, which are not shown in Figure 2 because their microstructures were not recorded.

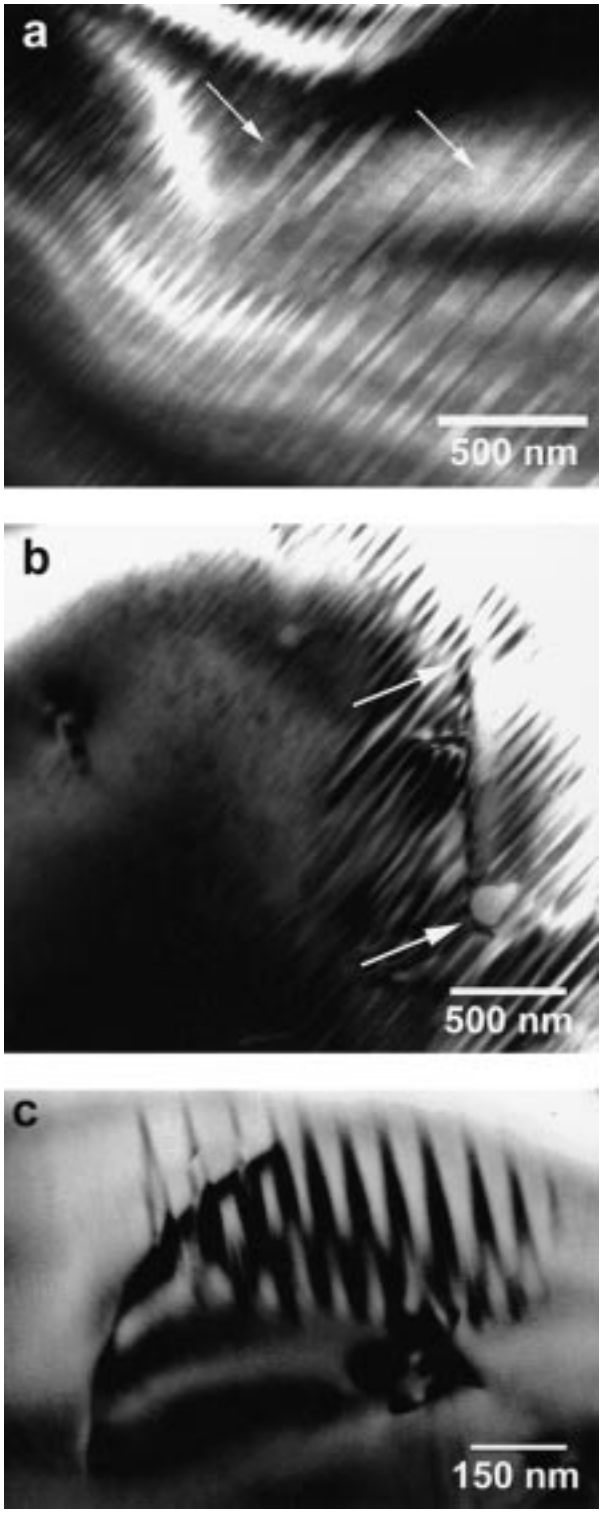

FIGURE 3. Exsolution lamellae. (**a**) (Spl 106c). Exsolution lamellae in $\sim An_{10-15}$. Multiple contrast fringes (examples at arrows) indicate unusually sharp planar boundaries observed in parts of this grain. (**b**) (Spl 106c). Lamellae become increasingly fine and diffuse approaching a fracture just outside the upper left corner of the image. Arrows show corners of an approximately square area where beam damage during AEM analysis was unusually severe, illustrating the typical size of an analysis area and its relationship to the lamellae. Areas with and without lamellae are both $\sim An_{10}$. (**c**) (Toce 76f). A small patch of lamellae in an otherwise crystallographically homogeneous area. The area with the lamellae may be slightly more calcic than adjacent areas without, although both are $\sim An_{3-4}$.

→

MICROSTRUCTURAL OBSERVATIONS

Figures 3 through 10 show representative exsolution microstructures. Although attempts were made to obtain AEM analyses and microstructural observations from the same areas, this was often impractical because of sample thickness or difficulties in finding exactly the same area with two different microscopes. Unless stated otherwise in figure captions, the compositions of the microstructures shown here were not measured. Areas shown in figures without chemical analyses are identified as peristerites primarily because of similarities between their microstructures and those in measured areas from the same sample, supplemented by some combination of qualitative chemical analyses, diffraction patterns, and proximity to measured areas. The relevant areas in the Mis 38a sample broke before any quantitative chemical analyses could be made, and are identified as peristerites based on similarity to microstructures in other grains from the same hand sample for which qualitative analyses were made, and on diffraction patterns from seven zone axes.

Lamellae

Lamellae occur as the only exsolution microstructure in regions several micrometers across in Toce 68c, Toce 76f, Spl 106c, Str 4179, and Sci 1649. Lamellae in intergrowths with tweeds occur in Toce 76f and Mis 38a, and are described below.

Although the edges of lamellae only rarely show multiple contrast fringes resulting from sharp crystallographic boundaries (Fig. 3a), changes in the appearance of the lamellae as the specimen is tilted indicate that they are essentially planar features. Ends of lamellae are typically gently tapering (e.g., Figs. 3b and 3c); however, some groups of lamellae end at dislocations or subgrain boundaries (Fig. 4). Dislocations were never observed at boundaries between lamellae or at the tapering ends of individual lamellae, suggesting that both the sides and the ends of the lamellae have a high degree of crystallographic coherence.

Lamellae are typically 15–35 nm thick. Finer, more diffuse, lamellae also were observed in some cases (e.g., central part of Fig. 3b). Although spacing is commonly consistent for at least several micrometers, locally it can be variable even in sharply bounded lamellae (e.g., compare the left and right sides of Fig. 3a). Branching, interconnected lamellae are common in some areas, and a few individuals curve or branch in even the most regular areas.

Selected area electron diffraction (SAED) patterns from areas with lamellae show conspicuous streaks perpendicular to the lamellae in the associated images. The streaks are continuous, and individual satellite reflections were not observed.

Tweeds

Tweeds that are the dominant microstructures in regions at least several micrometers across occur in Str 4179, Toce 76f, CT 15, and Vz 670, and are described here. Tweeds in intergrowths with lamellae occur in Toce 76f and Mis 38a, and are described later.

All of the tweeds in Str 4179 and the relatively calcic tweed in Toce 76f ($\sim An_{16}$, Fig. 2) have a distinctive appearance (Figs. 5a and 5b). One direction is quite conspicuous, and consists of short, somewhat irregularly spaced lamellae. The other is usually finer and more diffuse, and visible from a more restricted range of orientations. The coarseness and diffuseness of exsolution microstructures in both directions may vary significantly over distances of only a few micrometers (Fig. 5b).

In many cases, SAED patterns of the Str 4179 tweeds show obvious streaks perpendicular to one or both directions in the tweed. Numerous sharp, closely spaced satellite reflections may be visible in the streaks perpendicular to the coarser direction at the outer edges of SAED patterns. Similar reflections have been interpreted as representing the distribution of periodicities in the tweed (Korekawa et al. 1970; Nord et al. 1978).

TEM examination of two plagioclase grains from CT 15 suggests that both may be tweedy throughout. AEM analyses from one of the grains consistently show a composition of $\sim An_{15}$, whereas the other grain has tweeds of two distinct compositions ($\sim An_3$ and $\sim An_{15}$, Fig. 2). CT 15 tweeds of both compositions are characteristically fine and diffuse, and typically appear quite homogeneous over large areas of the specimen (Fig. 5c). The sodic tweeds are slightly coarser and less regular than the calcic tweeds only a few micrometers away; however, the two are sufficiently similar that they cannot be readily distinguished by appearance alone. Both CT 15 grains are highly deformed, and small phyllosilicate grains within the plagioclase are commonly shredded. The CT 15 tweeds generally did not produce streaks in SAED patterns; however, fine, diffuse streaks were observed perpendicular to the tweed directions in a few instances.

In many cases, dislocations do not appear to affect the morphologies of tweeds. However, locally highly irregular tweeds in some cases are found adjacent to subgrain boundaries (e.g., Fig. 6a, from CT 15) or in areas of high dislocation density (e.g., Fig. 6b, from Vz 670).

Intergrown tweeds and lamellae

Many of the lamellae in the Toce 76f and Mis 38a specimens are intergrown with areas of fine, diffuse tweeds. The tweeds and lamellae occur in patches with irregular, curving boundaries, some of which define narrow stripes several micrometers long (Figs. 7 and 8).

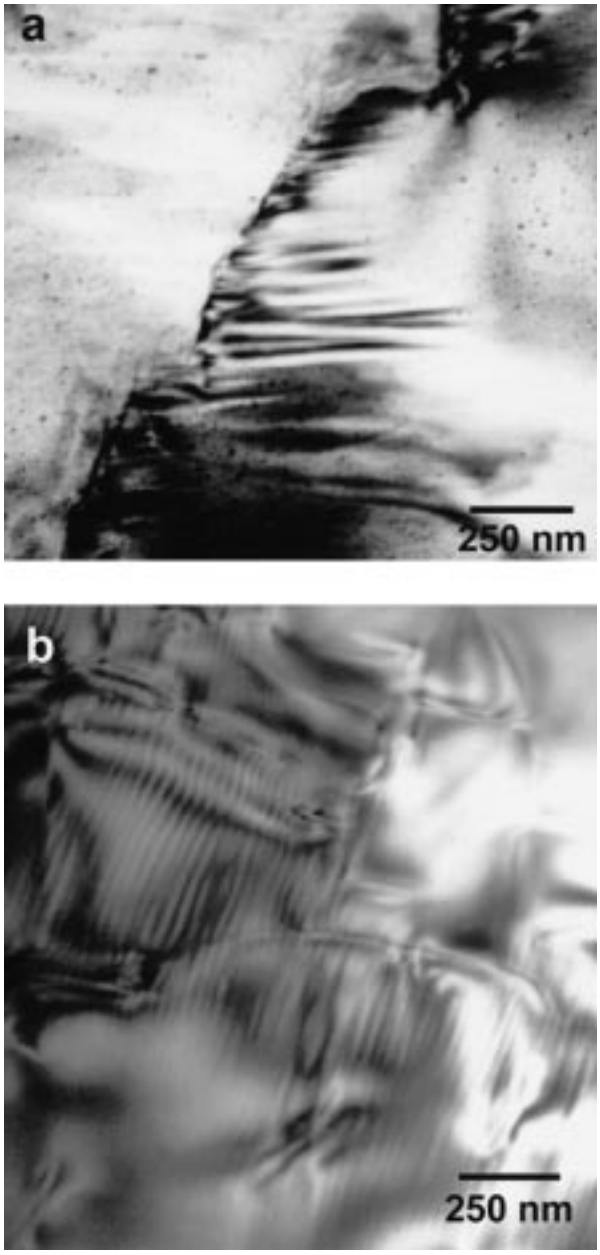

FIGURE 4. Ends of lamellae (excluding intergrowths with tweeds). (**a**) (Toce 76f). Lamellae extending away from a high-angle grain or subgrain boundary. The speckled appearance and white streaks from the upper left to the lower right are due to a very uneven carbon coat. (**b**) (Sci 1649). Lamellae extend away from dislocations, becoming increasingly diffuse until they can no longer be distinguished.

The widths and orientations of lamellae in intergrowths are indistinguishable from those of lamellae that occur as the only exsolution microstructures over large areas. Patches of lamellae adjacent to tweeds in Toce 76f are slightly more sodic than lamellae that occur as the only microstructure over large areas. Lamellae with well-defined sides and ends alternate with lamellae that have an

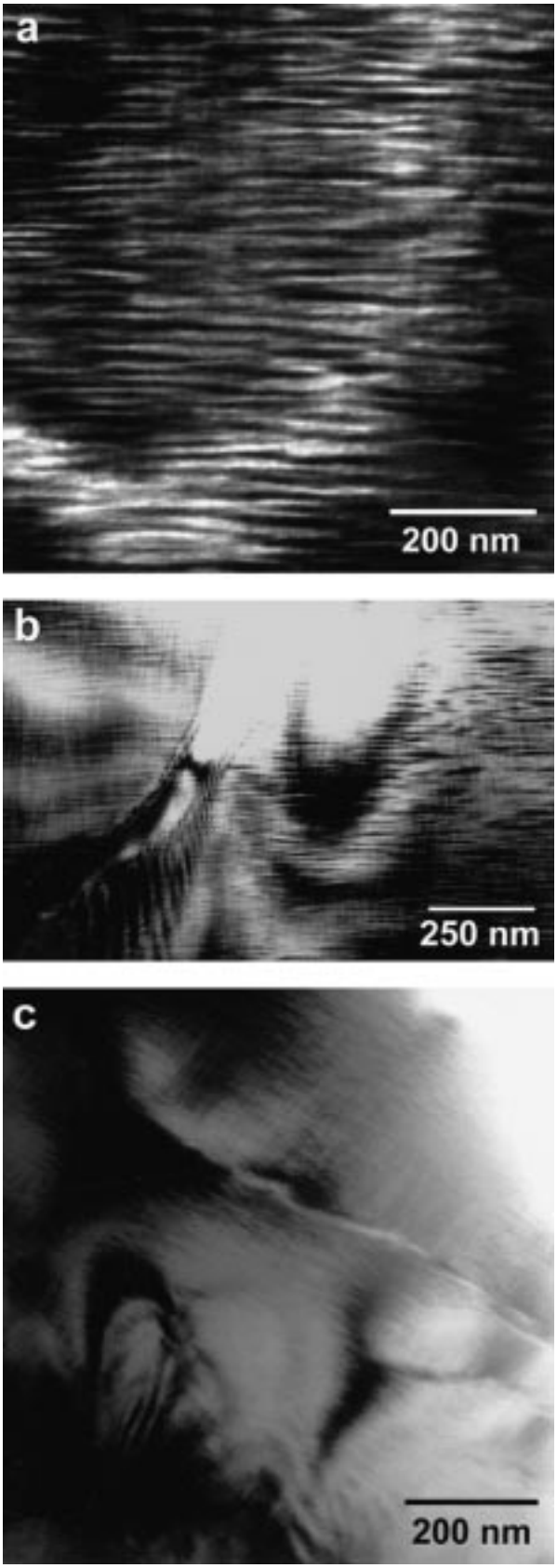

FIGURE 5. Tweeds. (**a**) (Str 4179) Typical tweeds from this specimen. One direction consists of short, highly interconnected lamellae; the other (approximately vertical on the page) is far finer and more diffuse. (**b**) (Str 4179) Note the difference in coarseness and uniformity of the tweeds in the upper left and right side. The conspicuous feature running from the top center to the lower left is a healed fracture; heavy vertical lines below it are probably moiré fringes. (**c**) (CT 15) Fine, diffuse, uniform tweeds occur over large areas of the CT-15 grains in this study. Nearby areas with similar exsolution microstructures are $\sim An_{15}$. ←

imperceptible transition into tweeds (Fig. 9). Areas with lamellae are very slightly more calcic than the adjacent tweeds (Fig. 2), suggesting that the well-defined lamellae may be oligoclase and the lamellae without recognizable ends may have at most a few mole percent anorthite.

Exsolution directions in the tweeds are approximately parallel and perpendicular to the lamellae (Figs. 7, 8, and 9). In almost all cases, the direction roughly perpendicular to the lamellae is far more conspicuous than the parallel direction, and usually appears less diffuse or more regular. This direction persists between widely spaced individuals in patches of lamellae for at least a short distance, whereas the parallel direction may not (Figs. 9 and 10).

SAED patterns from the fine tweeds show round spots without streaks. Streaks in SAED patterns from areas with lamellae, or with both tweeds and lamellae, are indistinguishable from those produced by lamellae that are not intergrown with tweeds.

Reflections near the outer edges of one very strongly exposed [001] SAED pattern from an area of intergrown tweeds and lamellae in Toce 76f are split, and have doubled streaks. These features are interpreted as arising from two reciprocal lattices with slightly different γ^* angles, similar to those that have been used to determine compositions of albite and oligoclase in exsolved peristerites using XRD (Baschek and Eberhard 1995 and older references therein). Similar features also may be present in less strongly exposed [001] patterns, but are difficult to identify because the appropriate reflections are fainter.

DISCUSSION

Exsolution mechanisms

Champness and Lorimer (1976) suggested that tweeds are the initial exsolution microstructures in all peristerite compositions, and that lamellae form by preferential coarsening of one direction in sodic peristerites and disappearance of the other. This conjecture would seem to require the existence of sodic tweeds and of intergrowths between tweeds and lamellae in appropriate specimens. Both of these were observed in this study.

As noted by previous researchers who have tentatively identified the lamellae as the result of spinodal decomposition, it is difficult or impossible to distinguish lamellae formed by spinodal decomposition from those formed by nucleation and growth once they have coarsened sig-

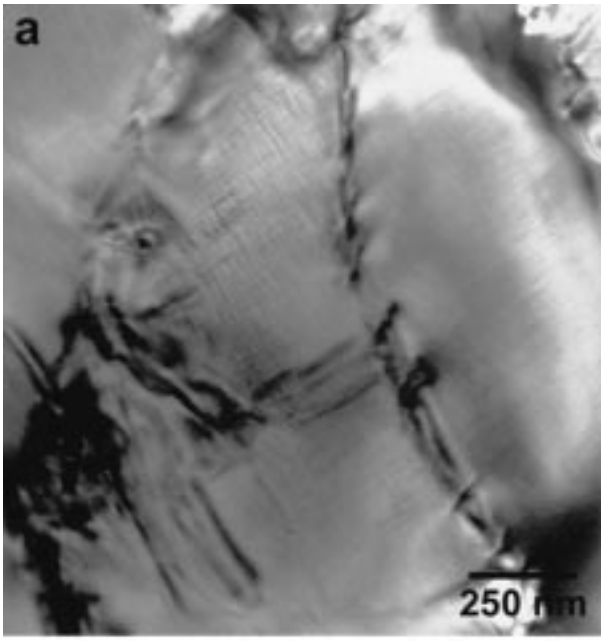

FIGURE 6. Irregular tweeds associated with deformation (**a**) (CT 15) Both directions of the tweed become coarser between two subgrain boundaries, without developing a single preferred direction. (**b**) (Vz 670) A highly deformed, irregular tweed. Arrows show dislocations.

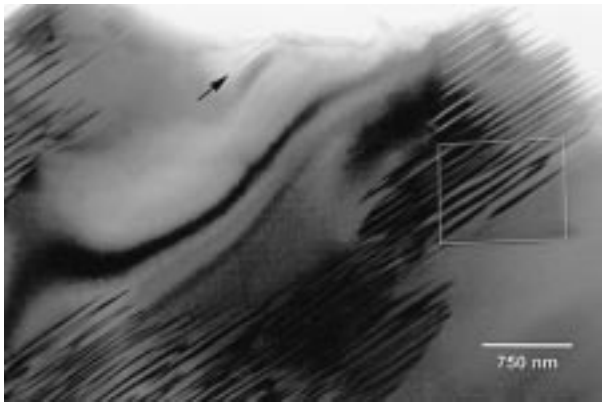

FIGURE 7. (Toce 76f) Patchy intergrowth of tweeds and lamellae. Composition is $\sim An_3$ in lamellae at upper left (measured just outside figure), $\sim An_2$ in central patch of tweeds, and $\sim An_4$ at border between right patch of lamellae and tweeds (area outlined by white box). Note the small group of short lamellae (arrow).

nificantly (e.g., Nord et al. 1978; Champness and Lorimer 1976). Crystallographic relationships between the two types of lamellae presumably would be similar, because in both cases they would minimize elastic strain energies due to differences in lattice parameters at the lamellae boundaries. Observations of lamellae without subgrain boundaries or other lattice discontinuities, or of lamellae and dislocations that appear unrelated to each other, are likewise inconclusive, because lamellae that have grown a substantial distance away from an initial heterogeneous nucleation site or a nucleation site outside the plane of the specimen could appear to be unrelated to deformation. If the exsolution microstructures have not coarsened significantly, however, lamellae formed by spinodal decomposition will have only one reciprocal lattice, while het-

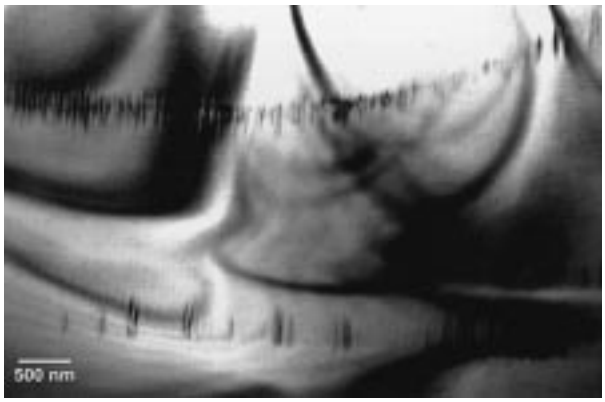

FIGURE 8. (Mis 38a) Two narrow bands of lamellae surrounded by tweeds (not visible in this orientation). The lower edge of the bottom band is bounded by a planar crystallographic feature, possibly a microtwin. Diffuse contrast fringes perpendicular to the lamellae in the left part of the upper band reflect small amounts of strain due to an unidentified crystallographic feature parallel to this part of the band.

FIGURE 9. (Toce 76f) Lamellae with well-defined ends in a matrix that passes imperceptibly into the tweeds in the lower right part of the image (direction parallel to the lamellae is out of contrast). Arrows show a very short lamella with two visible ends and a kinked lamella that is more diffuse near its tip. Note irregular spacing of the lamellae and slight difference in orientation between the top and bottom of the image.

erogeneously nucleated lamellae will have two from the very beginning (e.g., Champness and Lorimer 1976).

One of the problems raised by interpreting both the peristerite tweeds and lamellae as products of spinodal decomposition is that the previously reported composition of the calcic lamellae is outside the range of bulk compositions in which lamellae have been observed to form. If lamellae result from spinodal decomposition, then those formed in a bulk composition of $\sim An_7$, for example, must have progressed from an initial composition only slightly more calcic than that to their final composition of $\sim An_{25}$, passing through compositions of $\sim An_{18-20}$ in the process. At the same time, initial bulk compositions of $\sim An_{18}$ form tweeds, but are apparently unable to coarsen into lamellae. Although it has been speculated that the failure of the tweeds to coarsen is due to a competing tendency to form e-structures in the calcic end-members of the exsolution, the implications of this idea have not been rigorously addressed.

The observations reported here suggest that the relationship between the tweeds and lamellae is not simply coarsening. If the lamellae formed by coarsening of the tweeds, it seems likely that their orientation would be parallel to the more conspicuous tweed direction (approximately perpendicular to the orientation that actually occurs), and that there would be a continuous transition between the ends of lamellae and the lamellae-parallel direction in the tweeds. Instead, the data show that where lamellae end in tweeds, there is no appearance of continuity between the two microstructures (Figs. 9 and 10b). Adjacent tweedy and lamellar regions have slightly different compositions; thus, the lamellae cannot have formed simply by coarsening of the tweeds.

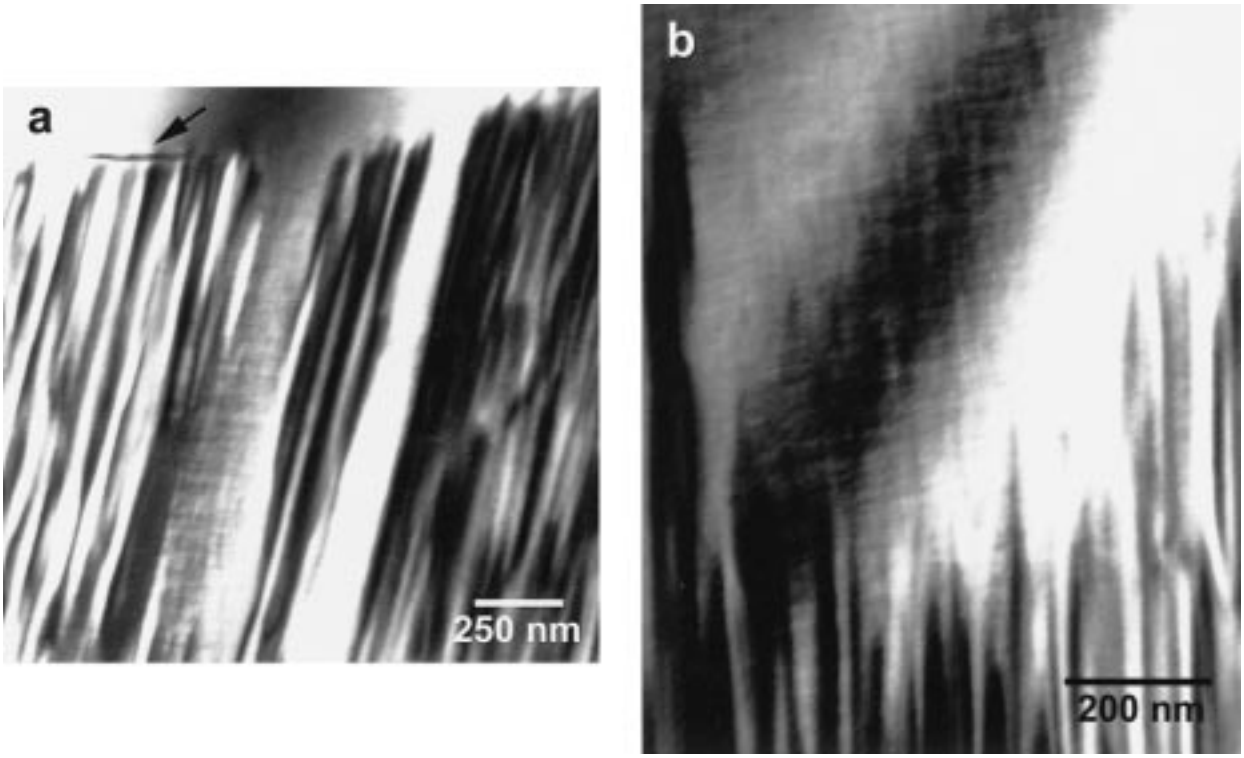

FIGURE 10. Details of relationships between tweeds and lamellae. (**a**) (Mis 38a) Lamellae end abruptly at what appears to be a composition boundary. The arrow indicates a dislocation along the boundary. Finer microstructures (possibly tweeds, although only the direction approximately perpendicular to the lamellae was identified) occur between some widely spaced lamellae, but not where spacing is closer. (**b**) (Mis 38a) The tapering ends of the group of lamellae on the left in **a,** again showing that at least one direction of the tweed extends into the areas between the lamellae.

Many of the characteristics of the lamellae can be explained more readily by heterogeneous nucleation. Figures 4 and 8 show lamellae with one end at a subgrain boundary or dislocation and the other in homogeneous crystal or tweeds. The often somewhat irregular spacing of the lamellae (Figs. 4, 8, 9, and 10) and presence of two reciprocal lattices are likewise more consistent with nucleation than with spinodal decomposition.

Patchy intergrowths of tweeds and lamellae on a scale of several micrometers seem likely to reflect compositional differences in the host plagioclase. Smaller-scale intergrowths, in which tweeds occur between widely spaced lamellae but not between more narrowly spaced ones, may suggest an exsolution process in which nucleation of relatively calcic lamellae depleted the immediately surrounding areas of calcium to produce albite. Areas between more widely spaced lamellae were not depleted. Sodic tweeds are inferred to form by spinodal decomposition in a narrowly defined compositional range between albite (which does not exsolve) and areas that are calcic enough for heterogeneous nucleation to be possible, given appropriate surfaces for nucleation.

Fine, diffuse, highly periodic tweeds and lamellae probably formed by spinodal decomposition. Tweeds like those from Str 4179 may also result from spinodal decomposition (Nord et al. 1978). These tweeds are more calcic than any composition that has been reported to form lamellae; consequently, it seems unlikely that they coarsen much further than the examples shown here.

Factors affecting microstructures

The observations in this study demonstrate a strong correlation between local composition and microstructures, suggesting that the plagioclases are quite well ordered. Transitions between tweeds and lamellae, and between lamellae and homogeneous areas, almost always occur together with compositional changes. Some more subtle distinctions, such as the differences in coarseness and regularity between the CT 15 sodic and calcic tweeds, are also correlated to composition.

In contrast, changes in the spacing of the lamellae could not be shown to reflect significant differences in the relative proportions of Ca, Al, and Si. Although it is possible that changes in spacing, like those seen in Figure 3a, are caused by compositional differences too small to be measured, they may instead reflect historical factors such as the original spacing of heterogeneously nucleated lamellae or geometries of migrating subgrain boundaries during deformation.

Previous regional studies in the Lepontine Alps have demonstrated that host-rock composition and metamorphic grade are important influences on the compositions of the plagioclase that forms in a particular rock (e.g., Wenk 1962; Wenk and Wenk 1984); but, once this composition has formed, neither the host-rock composition nor the metamorphic grade has a demonstrable influence on the microstructures observed here. There are certainly differences between individual samples with similar compositions from different host rocks and metamorphic grades. However, the microstructural differences between these samples in many cases are within the range of variability that can be observed within a single grain, and are certainly less than the observed variability between the different grains from the same hand sample.

Many of the microstructures studied here may have formed in an environment of simultaneous exsolution and dynamic recrystallization (perhaps explaining why they are so different from those reported in pegmatitic peristerites). The deformation microstructures and compositional patchiness in the grains studied here are similar to those produced during recrystallization of experimentally deformed albite-bytownite mixtures in the dislocation creep regime, where they have been interpreted as consequences of high-diffusivity zones along migrating subgrain boundaries (Yund and Tullis 1991). Observations of narrow, continuous regions with peristerite compositions and unusually high dislocation densities or closely spaced subgrain boundaries in more calcic plagioclases (Janney and Wenk, in preparation; Janney 1996) support a strong relationship between deformation and diffusion in the Alpine metamorphic plagioclase, as do the irregularly coarsened tweeds in Figure 6. Because Al-Si interdiffusion in plagioclase is very slow, it seems likely that relatively rapid local compositional changes along migrating subgrain boundaries may also lead to disequilibrium Al-Si ordering.

In conclusion, it should be emphasized that the sodic feldspars in this study were selected because they were large crystals whose optical characteristics suggested that they might contain compositional zoning. The observations of pervasive exsolution microstructures in these samples may not be representative of sodic metamorphic plagioclase in general. Microstructures are quite different in each of the grains presented here, and many observations are unique. It is likely that the range of peristerite exsolution microstructures in metamorphic plagioclase is wider than has been observed to date, perhaps even within the grains studied here.

Both lamellae and tweeds are common exsolution microstructures in Alpine metamorphic plagioclase with compositions from a few mole percent anorthite to $\sim An_{18}$. Lamellae occur in compositions more sodic than $\sim An_{10–15}$; tweeds occur throughout the entire range of exsolution microstructures. Lamellae are typically about 15–35 nm wide; occasional areas with far finer, more diffuse lamellae were also observed.

Chemical and microstructural observations of areas with intergrown tweeds and lamellae suggest that the relationship between the two is not one of preferential coarsening. Instead, it seems likely that lamellae form by heterogeneous nucleation in areas in which composition is favorable and there are appropriate sites, whereas tweeds form by spinodal decomposition.

Detailed AEM observations show compositional patchiness within many grains, and also show that compositional variations usually accompany variations in microstructures, such as the boundary between tweeds and lamellae.

ACKNOWLEDGMENTS

D.E.J. thanks the National Center for Electron Microscopy, Ernest Orlando Lawrence Berkeley National Laboratory for providing AEM instrumentation and training. She thanks Ian Carmichael and Ronald Gronsky (U.C. Berkeley) for serving on her dissertation committee, E. Wenk for providing samples and plagioclase composition data, and Ray and Joan Rogers for helpful conversations and hospitality during the writing of the first draft of this manuscript. She is also appreciative of financial support from a National Defense Science and Engineering Graduate Fellowship and a UC Berkeley Affirmative Action Dissertation-Year Fellowship. H.R.W. acknowledges support from NSF EAR-914605. We also thank Michael Carpenter and Bill Brown, whose perceptive review comments led to great improvements in the paper, and Adrian Brearley for his editorial handling.

REFERENCES CITED

Ashworth, J.R. and Evirgen, M.M. (1985) Plagioclase relations in pelites, central Menderes Massif, Turkey. I. The peristerite gap with coexisting kyanite. Journal of Metamorphic Geology, 3, 207–218.

Baschek, G. and Eberhard, E. (1995) Structural and chemical investigation of peristerites by transmission electron microscopy (TEM) and X-ray diffraction. European Journal of Mineralogy, 7, 309–317.

Brown, W.L. (1960) The crystallographic and petrologic significance of peristerite unmixing in the acid plagioclases. Zeitschrift für Kristallographie, 113, 330–344.

———(1989) Glide twinning and pseudotwinning in peristerite: Si,Al diffusional stabilization and implications for the peristerite solvus. Contributions to Mineralogy and Petrology, 102, 313–320.

Carpenter, M.A. (1981) A"conditional spinodal" within the peristerite miscibility gap of plagioclase feldspars. American Mineralogist, 66, 553–560.

———(1994) Subsolidus phase relations of the plagioclase feldspar solid solution. In I. Parson, Ed., Feldspars and their Reactions, NATO ASI Series, C421, p. 221–269. Kluwer Academic Publishers, Dordrecht.

Champness, P.E., and Lorimer, G.W. (1976) Exsolution in silicates. In H.-R. Wenk, Ed., Electron Microscopy in Mineralogy, p. 174–204. Springer-Verlag, Berlin.

Coward, M. and Dietrich, D. (1989) Alpine tectonics—an overview. In M. Coward, D. Dietrich, and R.G. Park, Eds., Alpine Tectonics, 45, p. 1–29. Geological Society, London.

Crawford, M.L. (1966) Composition of plagioclase and associated minerals in some schists from Vermont, U.S.A., and South Westland, New Zealand, with inferences about the peristerite solvus. Contributions to Mineralogy and Petrology, 13, 269–294.

Fleet, S.G. and Ribbe, P.H. (1965) An electron-microscope study of peristerite plagioclases. Mineralogical Magazine, 35, 165–176.

Frey, M., Bucher, K., Frank, E., and Mullis, J. (1980) Alpine metamorphism along the geotraverse Basel-Chiasso: a review. Eclogae geologicae Helvetica, 73, 527–546.

Frey, M., Hunziker, J.C., Jäger, E., and Stern, W.B. (1983) Regional distribution of white K-mica polymorphs and their phengite content in the Central Alps. Contributions to Mineralogy and Petrology, 83, 185–197.

Grapes, R. and Otsuki, M. (1983) Peristerite compositions in quartzofeldspathic schists, Franz Josef-Fox Glacier Area, New Zealand. Journal of Metamorphic Geology, 1, 47–61.

Hunziker, J.C., Desmons, J., and Martinotti, G. (1989) Alpine thermal evolution in the central and western Alps. In M. Coward, D. Dietrich, and R.G. Park, Eds., Alpine Tectonics, 45, p. 353–367. Geological Society of London.

Janney, D.E. (1996) Compositional microstructures in Alpine metamorphic plagioclases: a study by analytical and transmission electron microscopy. Ph.D. dissertation, University of California, Berkeley.

Korekawa, M., Nissen, H.-U., and Philipp, D. (1970) X-ray and electron-microscopic studies of a sodium-rich low plagioclase. Zeitschrift für Kristallographie, 131, 418–436.

Laves, F. (1954) The coexistence of two plagioclases in the oligoclase compositional range. Journal of Geology, 62, 409–411.

Lorimer, G.W., Nissen, H.-U., and Champness, P.E. (1974) High voltage electron microscopy of deformed sodic plagioclase from an Alpine gneiss. Schweizerische mineralogische und petrographische Mitteilungen, 54, 707–715.

Mackinnon, I.D.R. (1990) Low-temperature analyses in the analytical electron microscope. In I.D.R. Mackinnon and F.A. Mumpton, Eds., Electron-Optical Methods in Clay Science, CMS Workshop Lectures, vol. 2, p. 90–106. Clay Minerals Society, Boulder, Colorado.

Maruyama, S., Liou, J.G., and Suzuki, K. (1982) The peristerite gap in low-grade metamorphic rocks. Contributions to Mineralogy and Petrology, 81, 268–276.

McLaren, A.C. (1974) Transmission electron microscopy of the feldspars. In W.S. MacKenzie and J. Zussman, Eds., The Feldspars, p. 378–423. Manchester University Press, Manchester, U.K.

Miúra, Y. and Rucklidge, J.C. (1979) Ion microprobe analyses of exsolution lamellae in peristerites and cryptoperthites. American Mineralogist, 64, 1272–1279.

Nord, G.L. Jr., Hammarstrom, J., and Zen, E-a. (1978) Zoned plagioclase and peristerite formation in phyllites from southwestern Massachusetts. American Mineralogist, 63, 947–955.

Olsen, A. (1974) Schiller effects and exsolution in sodium-rich plagioclases. Contributions to Mineralogy and Petrology, 47, 141–152.

———(1975) Study of peristerites using transmission electron microscopy and energy dispersive X-ray analysis. Contributions to Mineralogy and Petrology, 51, 297–302.

Peacor, D.R. (1992) Analytical Electron Microscopy: X-Ray Analysis. In Mineralogical Society of America Reviews in Mineralogy, 27, 113–140.

Ribbe, P.H. and Smith, J.V. (1966) X-ray emission microanalysis of rock-forming minerals. IV. Plagioclase feldspars. Journal of Geology, 74, 217–233.

Smith, J.V. and Brown, W.L. (1988) Feldspar Minerals, vol. 1 (Second edition), 828 p. Springer-Verlag, Berlin.

Streckeisen, A. and Wenk, E. (1974) On steep isogradic surfaces in the Simplon area. Contributions to Mineralogy and Petrology, 47, 81–95.

Wenk, E. (1962) Plagioklas als Indexmineral in den Zentralalpen. Schweizerische mineralogische und petrographische Mitteilungen, 41, 311–319.

Wenk, H.-R. (1979) An albite-anorthite assemblage in low-grade amphibolite facies rocks. American Mineralogist, 64, 1294–1299.

Wenk, E. and Keller, F. (1969) Isograde in Amphibolitserien der Zentralalpen. Schweizerische mineralogische und petrographische Mitteilungen, 49, 157–198.

Wenk, E. and Wenk, H.-R. (1977) An-variation and intergrowths of plagioclases in banded metamorphic rocks from Val Carecchio (Central Alps). Schweizerische mineralogische und petrographische Mitteilungen, 57, 41–57.

———(1984) Distribution of plagioclase in carbonate rocks from the Tertiary metamorphic belt of the Central Alps. Bulletin de Minéralogie, 107, 357–368.

Wenk, H.-R., Hsaio, J., Flowers, G., Weibel, M., Ayranci, B., and Fejér, Z. (1977) A geochemical survey of granitic rocks in the Bergell Alps. Schweizerische mineralogische und petrographische Mitteilungen, 57, 233–265.

Wenk, E., Schwander, H., and Wenk, H.-R. (1991) Microprobe analyses of plagioclases from metamorphic carbonate rocks of the Central Alps. European Journal of Mineralogy, 3, 181–191.

Wruck, B., Salje, E.K.H., and Graeme-Barber, A. (1991) Kinetic rate laws derived from order parameter theory IV: Kinetics of Al, Si disordering in Na-feldspars. Physics and Chemistry of Minerals, 17, 700–710.

Yund, R.A. and Tullis, J. (1991) Compositional changes of minerals associated with dynamic recrystallization. Contributions to Mineralogy and Petrology, 108, 346–355.

MANUSCRIPT RECEIVED DECEMBER 3, 1997
MANUSCRIPT ACCEPTED OCTOBER 20, 1998
PAPER HANDLED BY ADRIAN J. BREARLEY